LETTER

doi:10.1038/nature10651

Messinian salinity crisis regulated by competing tectonics and erosion at the Gibraltar arc

D. Garcia-Castellanos[1] & A. Villaseñor[1]

The Messinian salinity crisis[1,2] (5.96 to 5.33 million years ago) was caused by reduced water inflow from the Atlantic Ocean to the Mediterranean Sea resulting in widespread salt precipitation and a decrease in Mediterranean sea level of about 1.5 kilometres due to evaporation[3]. The reduced connectivity between the Atlantic and the Mediterranean at the time of the salinity crisis is thought to have resulted from tectonic uplift of the Gibraltar arc seaway and global sea-level changes, both of which control the inflow of water required to compensate for the hydrological deficit of the Mediterranean[1,4]. However, the different timescales on which tectonic uplift and changes in sea level occur are difficult to reconcile with the long duration of the shallow connection between the Mediterranean and the Atlantic[5] needed to explain the large amount of salt precipitated. Here we use numerical modelling to show that seaway erosion caused by the Atlantic inflow could sustain such a shallow connection between the Atlantic and the Mediterranean by counteracting tectonic uplift. The erosion and uplift rates required are consistent with previous mountain erosion studies, with the present altitude of marine sediments in the Gibraltar arc[6,7] and with geodynamic models suggesting a lithospheric slab tear underneath the region[8–10]. The moderate Mediterranean sea-level drawdown during the early stages of the Messinian salinity crisis[3,5] can be explained by an uplift of a few millimetres per year counteracted by similar rates of erosion due to Atlantic inflow. Our findings suggest that the competition between uplift and erosion can result in harmonic coupling between erosion and the Mediterranean sea level, providing an alternative mechanism for the cyclicity observed in early salt precipitation deposits and calling into question previous ideas regarding the timing of the events that occurred during the Messinian salinity crisis[1].

It is broadly accepted that the period of widespread salt precipitation in the Mediterranean known as the Messinian salinity crisis (MSC) spanned from 5.96 to 5.33 Myr ago[1,2]. Although there is debate on how the events recorded in strata correlate between the marginal shallow basins and the deeper parts of the Mediterranean, biostratigraphic analyses[2,11] agree on the occurrence of two stages in both environments: stage 1 encompasses the early salt precipitation (forming the lower evaporites), producing massive gypsum deposits at the basin margins and involving minor sea-level drawdown; stage 2 includes the formation of the upper evaporites and Lago Mare deposits, and a kilometre-scale Mediterranean sea-level drop evidenced by the widespread presence of Messinian erosion surfaces[11]. During stage 2, the largest rivers flowing to the nearly desiccated Mediterranean excavated canyons about 2,500 m deep in the Nile delta[12] and 1,000 m deep at the mouth of the Rhone[13]. Strontium isotope data[14] indicate that stage 1 took place in a restricted Mediterranean, that is, one with reduced connectivity with the Atlantic, whereas stage 2 occurred in predominantly continental waters with little or no connection to the ocean. The durations of these two phases have been estimated at 360 and 270 kyr, respectively, on the basis of the assumption that the 14 to 17 cycles observed in the gypsum of stage 1 are due to Milankovitch precessional cycles of insolation.

Three mechanisms have been proposed as responsible for the closure of the seaways. A global sea-level drop can be discarded because the open-ocean benthic $^{18}O/^{16}O$ ratio, a proxy for glacio-eustasy, does not match the onset of evaporite deposition[1,15]. Similarly, no evidence has yet linked local tectonic fault deformation[16] along the corridors to the onset of the MSC, a period when tectonic activity was relatively low both in the Betic[17] and the Rifean corridors[18]. Accordingly, a long-wavelength, mantle-sourced tectonic uplift of the Betic and/or Rif mountains[6,18–21] is seen as the most plausible cause for the isolation of the Mediterranean[9], and is supported by the presence of uplifted, pre-Messinian marine sediments near the seaways in the Rif[6,18] and the Betics[7,19]. However, the physical feasibility of this mechanism has not yet been quantitatively tested, because former models of the MSC[4,21,22] predefined the connectivity conditions at the seaway. Because sea level varies on much shorter timescales than tectonic uplift, previous attempts at linking both processes[5] predict a succession of short desiccations and floods during both stages of the MSC. This may explain the large amount of salt precipitated during the MSC[3,22–24], which requires the evaporation of about 50 times the volume of the Mediterranean, but is in conflict with the notion of a two-stage MSC. Furthermore, the erosion produced by each flood would deepen and widen the inflow channel[25,26], implying a succession of multiple tectonic uplift and subsidence episodes[20,26] for which no geodynamic mechanism is known.

The alternative to multiple flooding is a long period of continuous inflow and limited outflow caused by a shallow connection between the Mediterranean and the Atlantic. This does not imply a large sea-level drawdown in the Mediterranean during stage 1, and allows for the required amount of salt to be precipitated in a few hundred thousand years. However, to avoid both interoceanic mixing and complete disconnection[5] this mechanism would require a fortuitous, *ad hoc* evolution of both sea level and uplift closely following each other with a deviation of only a few tens of metres[4]. Here we postulate that such a long-lasting, shallow connection can be naturally sustained by a competition between the tectonic obstruction of the seaway and its erosional deepening by water inflow, and that this competition was responsible for the salt precipitation during the first stage of the MSC.

To test this hypothesis, we combine a model of rock erosion with classical hydrodynamic equations and a climate-based water budget (Fig. 1 and Supplementary Methods) to calculate the timing of water and salt flow between the Atlantic and the Mediterranean and the erosion produced along the connecting corridor. The evolution of the reference model in Fig. 2 starts with a 60-m-deep seaway that is uplifted at a constant rate. As the seaway becomes shallower, less water is able to cross the strait, and the Mediterranean sea level decreases evaporatively. When the seaway becomes shallower than a few tens of metres, the Mediterranean sea level decreases at rates of centimetres per year. As this sea-level difference across the Gibraltar arc increases, so does the shear stress of the inflow and the associated seaway erosion rate, which eventually compensates the imposed uplift rate. This keeps the inlet neither open enough to allow double circulation nor completely closed. If the uplift rate exceeds a critical value, U_c, then it overcomes erosion and the threshold rises above global sea level, cancelling the

[1]Instituto de Ciencias de la Tierra Jaume Almera, CSIC, Solé i Sabarís s/n, 08028 Barcelona, Spain.

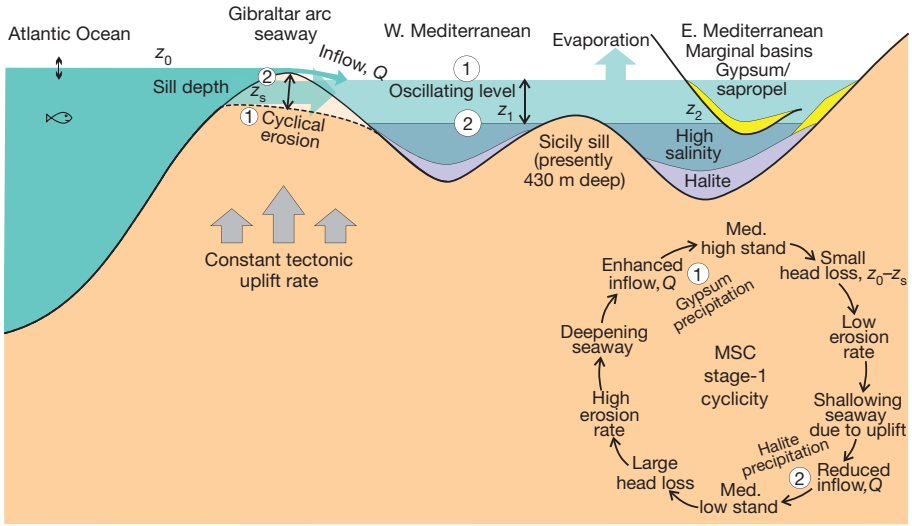

Figure 1 | Competition between uplift and erosion along the last corridor connecting the Atlantic and the Mediterranean during stage 1 of the MSC. Erosion at the sill is controlled by rock erodibility and water inflow, which is calculated as a function of sill depth, $z_0 - z_s$, and head loss, $z_0 - z_1$. Oscillations in water level and salinity can result from feedback (harmonic coupling) between tectonic uplift, water flow, evaporation and sill erosion. Sketch not drawn to scale.

connection permanently. The reference model in Fig. 2 corresponds to the critical uplift rate (4.9 mm yr^{-1}) for the reference erodibility and climatic parameters. We searched systematically for the critical uplift rates for a range of erodibility values consistent with previous river incision studies (Fig. 3) and found that values greater than 1 mm yr^{-1} are needed. These values are close to uplift rates expected from mantle geodynamic models simulating slab detachment[9,10]. Critical uplift rates are also dependent on the hydrological deficit. Changing the climatic

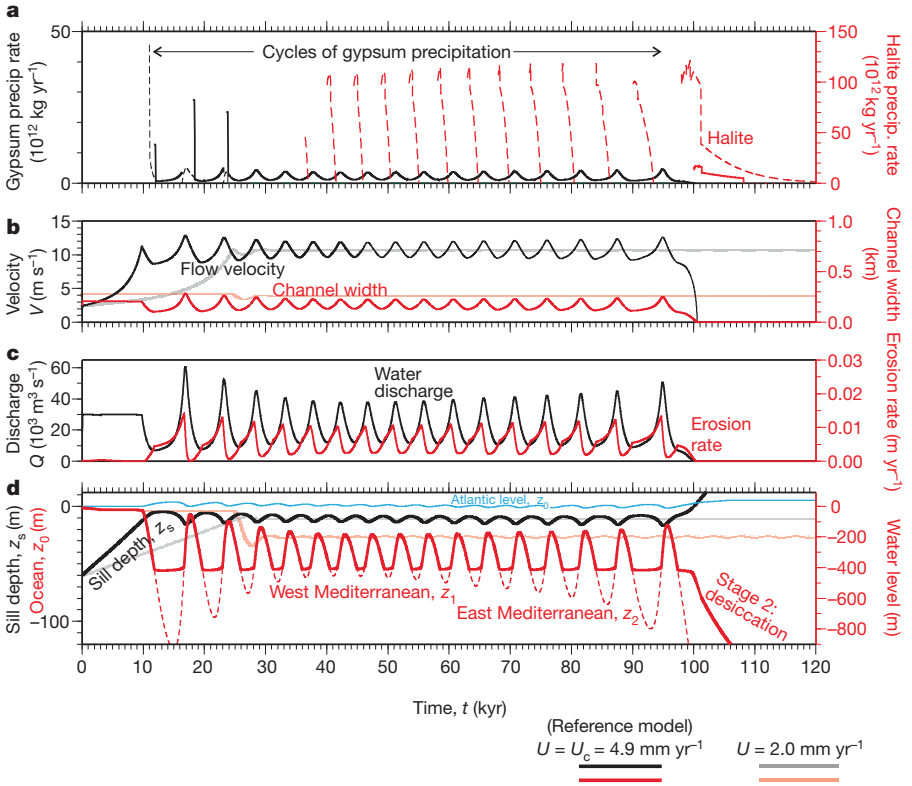

Figure 2 | Calculated evolution of the reference model resulting from competition between seaway uplift and erosion. The uplift rate is set to $U = 4.9$ mm yr^{-1}, close to the critical value causing complete disconnection, and undergoes a minor acceleration to force the formation of exactly 17 precipitation cycles before closure at $t = 100$ kyr. The model starts with a 60-m-deep seaway at $t = 0$. At $t = 11$ and $t = 12$ kyr, the saturation of gypsum is reached in the eastern and western Mediterranean, respectively. **a**, Halite and gypsum precipitation rates; **b**, flow velocity and width of the seaway; **c**, inflow water discharge and erosion at the seaway; **d**, seaway depth (black), level of the Atlantic (blue), and level of the Mediterranean (red). At $t = 10$ kyr, the seaway becomes shallow enough to reduce water discharge and velocity, allowing a Mediterranean evaporative drawdown that leads to higher slope and erosion along the seaway. The subsequent oscillations in sea level and salt precipitation are the result of dynamic harmonic coupling between the drawdown and the refill triggered when erosion deepens the seaway. The amplitude of sea-level oscillations in this example is an upper limit. For comparison, the results obtained for an uplift rate of 2.0 mm yr^{-1} are also displayed, by lighter lines, in **b** and **d**. Dashed lines in **a** and **d** indicate values for the eastern Mediterranean.

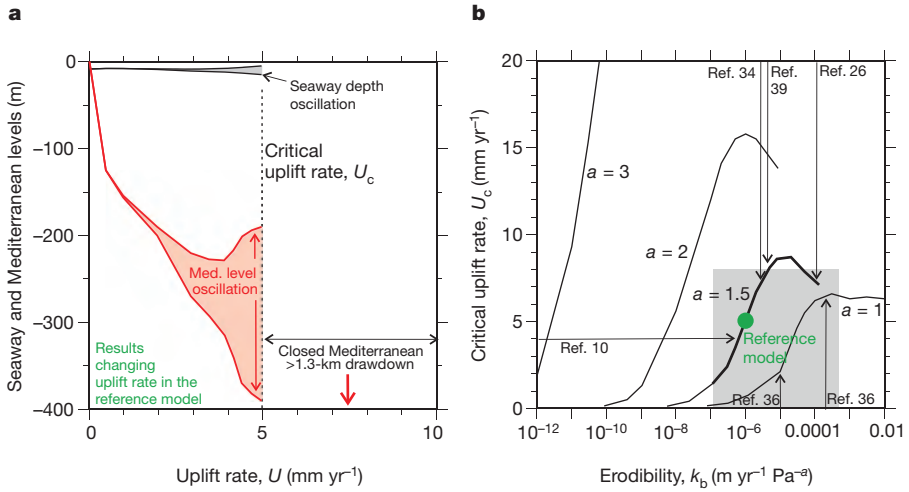

Figure 3 | Parameterization of the competition between uplift and erosion. **a**, Depth of the seaway and the Mediterranean sea level, and their range of oscillation as the seaway uplift rate approaches its critical value, U_c, at which there is complete disconnection from the Atlantic. **b**, Critical uplift rates required for closure, for a range of values of erodibility and for four values of the exponent, a, of the erosion power law. Labelled arrows indicate references for erodibility and uplift rates (for some references, see Supplementary Information). The grey-shaded area indicates the parameter ranges supported by the references and the model results.

conditions used for the calculations, from the relatively wet setting deduced for the MSC[27] to the present dryer conditions, implies an increase of the critical uplift rate by a factor of almost three. Thus, a relatively humid climate during the early Messinian may have facilitated the isolation and eventual evaporation of the Mediterranean by decreasing the amount of water crossing and eroding the seaway.

We found that uplift rates only slightly lower than the critical value produce a cyclic change in the sea level of the Mediterranean, even if uplift occurs at a constant rate. The dynamic equilibrium between uplift and erosion attained at low uplift rates develops into an apparent sea-level harmonic oscillation for values comparable to U_c. This happens as follows (Fig. 1). Inflow reduction by tectonic uplift leads to a delayed evaporative drawdown in the Mediterranean, with the time lag depending on the sea's hydrological deficit. The drawdown induces greater flow energy in the corridor and larger incision rates that deepen the seaway, allowing more water inflow and the recovery of the normal Mediterranean sea level. This reduction in sea-level difference leads to slower inflow and erosion that can be again overcome by tectonic uplift. This cyclic process produces salt precipitation and sea-level cycles of higher intensity as the uplift rate gets closer to the critical value (Fig. 3a). The period of these cycles is dependent on uplift rate and on the hydrological deficit, and using climatic parameters closer to the present drier climate scenario produces a reduction in the oscillation period by a factor of two relative to the reference model. This suggests that the cyclicity of the lower evaporites (stage 1) might be a result of the competition between tectonic uplift and water flow erosion, rather than of Milankovitch insolation changes as previously proposed[1]. In that case, the duration of stage 1 may have been half of previous estimates[1] or less, because the cycle periods that we obtain ($<$10 kyr) are less than half of the precession cycle (21 kyr). The uncertainty in erodibility and uplift data does not allow us definitively to state this as an origin for the cycles on the basis of only modelling techniques, and global sea-level changes might also have modulated shorter-term sediment sequences[4]. However, within the approaches taken here the coupling between uplift and erosion is dominant as long as global oscillations are smaller than about 10 m (Supplementary Fig. 3).

Regardless of the origin of the cycles, the results imply that stage 1 was sustained by a competition between uplift and erosion at the seaway, allowing for limited but uninterrupted Atlantic inflow. This is consistent with the observation that the Mediterranean underwent relatively small sea-level drawdown, of a few hundred meters or less[3], during stage 1, allowing the formation of coastal erosional surfaces[28]. During stage 2, any possible water supply from the Atlantic could not last more than a few thousand years because the large head loss across the Betic–Rifean orogen would imply high incision rates and lead irreversibly to a complete refill[26], leading back to the initial pre-MSC situation. Therefore, the simplest picture consistent with the physics of our model includes, first, a single stage of sustained inflow of Atlantic waters and limited or no outflow (stage 1), then a single stage of complete disconnection and kilometric drawdown with sea level controlled mainly by changes in the Mediterranean hydrological budget (stage 2), and then a single, final flood (Supplementary Fig. 1).

Evidence for the tectonic uplift required by the model is found near the last corridors connecting both oceanic domains. In the Betic internal basins, the pre-Messinian marine–continental transition is at present at altitudes close to 1,000 m (Fig. 4), with most intramountain basins emerging between 7.6 and 5.3 Myr ago[7]. In the Rifean corridor, palaeodepth reconstructions indicate a rapid shallowing starting 7.2 Myr ago at rates as high as 3.6 mm yr^{-1}, with the transition from marine to continental deposits occurring by 6.0 Myr ago[18] and lying at present at an altitude higher than 600 m. This is consistent with a long-wavelength uplift of at least that amount across the Rif–Atlas corridor[6,18]. Either of these uplifts can explain the closure of the Mediterranean according to the model presented here, which requires uplift of more than 1 mm yr^{-1} (Fig. 3b) over a period of at least 80 kyr.

Lithospheric slab detachment and roll back has previously been suggested as the possible cause for uplift that initiated the MSC[9]. Our model allows to bridge the gap quantitatively between such geodynamic processes and the MSC events. Slab detachment models predict uplifts of kilometre scale, with uplift rates ranging from 0.07 mm yr^{-1} (ref. 29) to 4 mm yr^{-1} (ref. 10). The higher values within this range are consistent with the rates needed to close the seaway in our model. Moreover, tear propagation of a hanging lithospheric slab underneath the Gibraltar arc[8] provides a mechanism of westwards propagation of both uplift and subsidence (Fig. 4). Recent seismic tomography obtained from the inversion of P-wave arrival times[30] supports the presence of such lithospheric tearing (Fig. 4 and Supplementary Information). The location of this tear point between the last pre-Messinian corridor and the strait of Gibraltar (Fig. 4) could explain the uplift and closure of the Betic seaways[9], and a later subsidence in Gibraltar, leading to the Zanclean flood[26]. But other modes of tectonic uplift cannot be completely ruled out as responsible for the closure of the Mediterranean: the ongoing tectonic convergence between Europe and Africa (about 4 mm yr^{-1} since the Tertiary

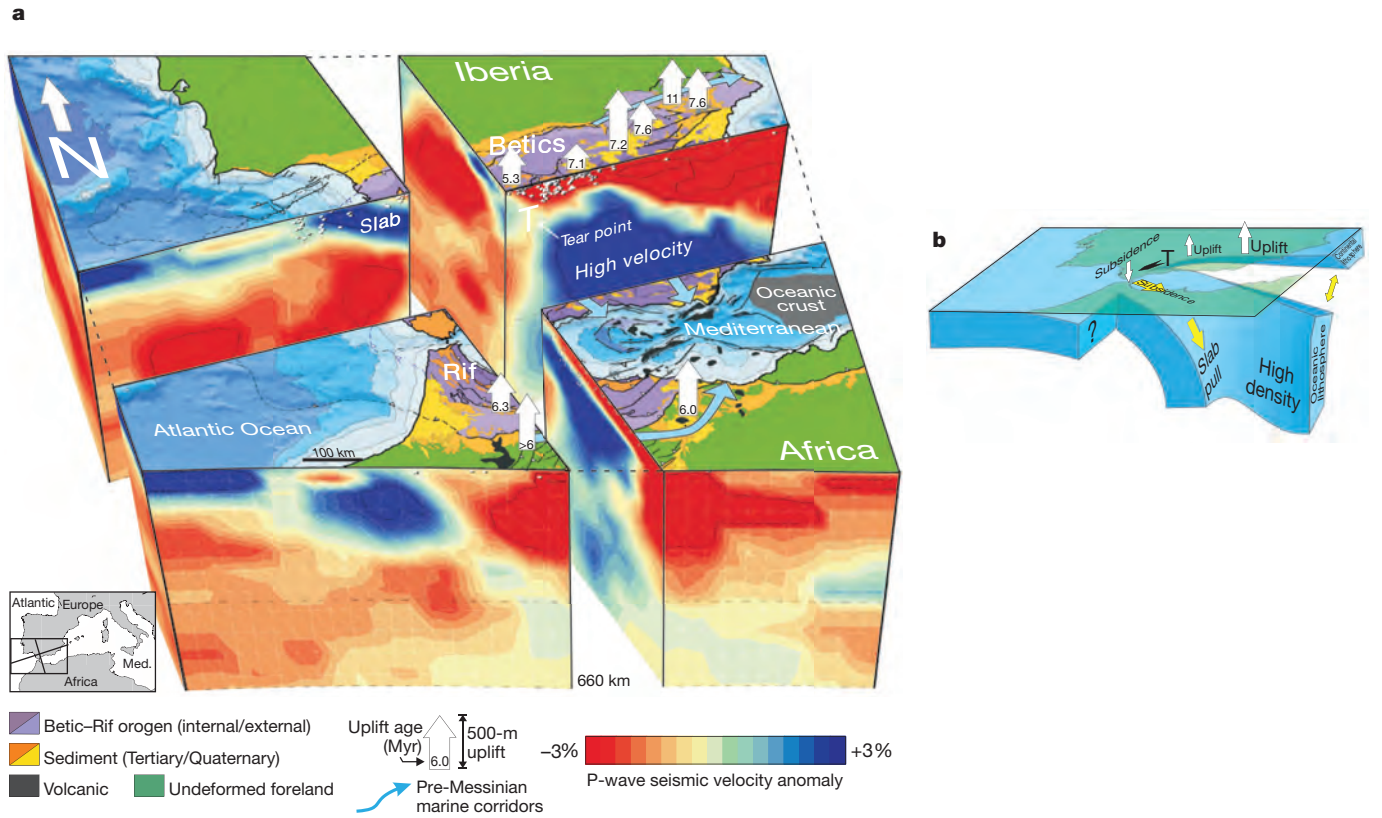

Figure 4 | Geodynamic interpretation of the results invokes the lateral migration of a tearing[8] of the lithospheric slab originally attached to the south Iberian margin. **a**, Geological map of the Gibraltar arc and subjacent mantle structure derived from seismic tomography. White arrows indicate uplift of intramountain basins within the Betics[7,19] and the Rif[6,18], and ages of their transition from marine to continental conditions[7]. White dots locate earthquake hypocentres used for the tomographic inversion and blue arrows locate proposed connecting corridors. **b**, Interpretative sketch: T marks the proposed lithosphere tearing point, separating areas where the sinking lithospheric slab (blue) is detached from Iberia, inducing surface uplift (to the east), from areas where it remains attached to the crust (to the west).

period) could also have contributed to uplift rates through faulting or doming[7].

The MSC has implications beyond its effects on the Mediterranean landscape. During stage 1, the Mediterranean basin sequestered about 10% of the salt of Earth's oceans, raising its freezing point by about 0.2 °C. During desiccation (stage 2), the evaporated Mediterranean waters were redistributed through the atmosphere to the world oceans, raising global sea level by about 10 m, as recorded in reef stratigraphy in the Pacific Ocean[31]. However, the climatic impact of the MSC remains elusive, as model results are ambiguous[27,32] and not well reflected in palynological data[33]. Final evidence on the timing and magnitude of these events may come in future from improved global climate models that could in turn benefit from the uniquely extreme conditions imposed by the Messinian natural laboratory.

METHODS SUMMARY

We calculate sea-level changes in the Mediterranean by developing a one-dimensional model of the depth of the seaway that limits the water inflow from the Atlantic. The feedback between water-flow-controlled incision and seaway-depth-controlled water flow is implemented by developing a formulation based on previous river incision studies and on standard hydrodynamic formulae. The model is based on the assumption that the depth of the seaway, z_s, depends on uplift and erosion, the last being a power-law function of basal shear stress. The level of the Mediterranean is a function of precipitation, evaporation, river supply and Atlantic inflow along the seaway. The evaporation surface of the Mediterranean is calculated as a function of its level, using a reconstructed hypsometry[21]. The interplay between tectonic uplift, incision and the driving role of hydraulic gradient across the seaway (resulting from the competition between inflow through Gibraltar and the water deficit in the Mediterranean) is calculated using an explicit finite-difference, time-iterative technique. At each time step, the water discharge, Q, is calculated on the basis of the depth of the sill and the head loss, and then seaway erosion is calculated from the basal shear stress of the flow. See Methods for further details.

Full Methods and any associated references are available in the online version of the paper at www.nature.com/nature.

Received 22 February; accepted 6 October 2011.

1. Krijgsman, W., Hilgen, F. J., Raffi, I., Sierro, F. J. & Wilson, D. S. Chronology, causes and progression of the Messinian salinity crisis. *Nature* **400,** 652–655 (1999).
2. Briand, F. (ed.) *The Messinian Salinity Crisis from Mega-Deposits to Microbiology – A Consensus Report* (CIESM Workshop Monographs 30, CIESM, 2008).
3. Hsü, K. J., Ryan, W. B. F. & Cita, M. B. Late Miocene desiccation of the Mediterranean. *Nature* **242,** 240–244 (1973).
4. Rohling, E. J., Schiebel, R. & Siddall, M. Controls on Messinian Lower Evaporite cycles in the Mediterranean. *Earth Planet. Sci. Lett.* **275,** 165–171 (2008).
5. Gargani, J. & Rigollet, C. Mediterranean sea level variations during the Messinian salinity crisis. *Geophys. Res. Lett.* **34,** L10405 (2007).
6. Babault, J., Teixell, A., Arboleya, M. L. & Charroud, M. A late Cenozoic age for long-wavelength surface uplift of the Atlas Mountains of Morocco. *Terra Nova* **20,** 102–107 (2008).
7. Iribarren, L., Vergés, J. & Fernàndez, M. Sediment supply from the Betic-Rif orogen to basins through Neogene. *Tectonophysics* **475,** 68–84 (2009).
8. Spakman, W. & Wortel, M. J. R. in *The TRANSMED Atlas: The Mediterranean Region from Crust to Mantle* (eds Cavazza, W. *et al.*) 31–52 (Springer, 2004).
9. Duggen, S., Hoernie, K., Van den Bogaard, P., Rüpke, L. & Morgan, J. P. Deep roots of the Messinian salinity crisis. *Nature* **422,** 602–606 (2003).
10. Andrews, E. R. & Billen, M. I. Rheologic controls on the dynamics of slab detachment. *Tectonophysics* **464,** 60–69 (2009).
11. Clauzon, G., Suc, J.-P., Gautier, F., Berger, A. & Loutre, M.-F. Alternate interpretation of the Messinian salinity crisis: controversy resolved? *Geology* **24,** 363–366 (1996).
12. Barber, P. M. Messinian subaerial erosion of the proto-Nile Delta. *Mar. Geol.* **44,** 253–272 (1981).
13. Clauzon, G. The Messinian Var canyon (Provence, southern France): paleogeographic implications. *Mar. Geol.* **27,** 231–246 (1978).

14. Flecker, R. & Ellam, R. M. Identifying late Miocene episodes of connection and isolation in the Mediterranean-Paratethyan realm using Sr isotopes. *Sedim. Geol.* **188–189,** 189–203 (2006).
15. Hilgen, F., Kuiper, K., Krijgsman, W., Snel, E. & van der Laan, E. Astronomical tuning as the basis for high resolution chronostratigraphy: the intricate history of the Messinian Salinity Crisis. *Stratigraphy* **4,** 231–238 (2007).
16. Weijermars, R. Neogene tectonics in the Western Mediterranean may have caused the Messinian salinity crisis and an associated glacial event. *Tectonophysics* **148,** 211–219 (1988).
17. Comas, M. C., Platt, J. P., Soto, J. I. & Watts, A. B. The origin and tectonic history of the Alboran Basin. *Proc. ODP Sci. Res.* **161,** 555–580 (1999).
18. Krijgsman, W. Late Neogene evolution of the Taza-Guercif Basin (Rifean Corridor; Morocco) and implications for the Messinian salinity crisis. *Mar. Geol.* **153,** 147–160 (1999).
19. Garcés, M., Krijgsman, W. & Agustí, J. Chronology of the late Turolian deposits of the Fortuna basin (SE Spain): implications for the Messinian evolution of the eastern Betics. *Earth Planet. Sci. Lett.* **163,** 69–81 (1998).
20. Govers, R. Choking the Mediterranean to dehydration: the Messinian salinity crisis. *Geology* **37,** 167–170 (2009).
21. Meijer, P., Th. & Krijgsman, W. A quantitative analysis of the desiccation and re-filling of the Mediterranean during the Messinian Salinity Crisis. *Earth Planet. Sci. Lett.* **240,** 510–520 (2005).
22. Blanc, P.-L. Improved modelling of the Messinian Salinity Crisis and conceptual implications. *Palaeogeogr. Palaeoclimatol. Palaeoecol.* **238,** 349–372 (2006).
23. Rouchy, J.-M. & Saint Martin, J. P. Late Miocene events in the Mediterranean as recorded by carbonate-evaporite relations. *Geology* **20,** 629–632 (1992).
24. Ryan, W. B. F. Decoding the Mediterranean salinity crisis. *Sedimentology* **56,** 95–136 (2009).
25. Blanc, P.-L. The opening of the Plio-Quaternary Gibraltar Strait: assessing the size of a cataclysm. *Geodin. Acta* **15,** 303–317 (2002).
26. Garcia-Castellanos, D. *et al.* Catastrophic flood of the Mediterranean after the Messinian Crisis. *Nature* **462,** 778–781 (2009).
27. Gladstone, R., Flecker, R., Valdes, P., Lunt, D. & Markwick, P. The Mediterranean hydrologic budget from a Late Miocene global climate simulation. *Palaeogeogr. Palaeoclimatol. Palaeoecol.* **251,** 254–267 (2007).
28. Just, J., Hübscher, C., Betzler, C., Lüdmann, T. & Reicherter, K. Erosion of continental margins in the Western Mediterranean due to sea-level stagnancy during the Messinian Salinity Crisis. *Geo-Mar. Lett.* **31,** 51–64 (2011).
29. Gerya, T. V., Yuen, D. A. & Maresch, W. V. Thermomechanical modelling of slab detachment. *Earth Planet. Sci. Lett.* **226,** 101–116 (2004).
30. Villaseñor, A., Spakman, W. & Engdahl, E. R. Influence of regional travel times in global tomographic models. *Geophys. Res. Abstr.* **5,** abstr. EAE03-A-08614 (2003).
31. Aharon, P., Goldstein, S. L., Wheeler, C. W. & Jacobson, G. Sea-level events in the South Pacific linked with the Messinian salinity crisis. *Geology* **21,** 771–775 (1993).
32. Schneck, R., Micheels, A. & Mosbrugger, V. Climate modelling sensitivity experiments for the Messinian Salinity Crisis. *Palaeogeogr. Palaeoclimatol. Palaeoecol.* **286,** 149–163 (2010).
33. Fauquette, S. *et al.* How much did climate force the Messinian salinity crisis? Quantified climatic conditions from pollen records in the Mediterranean region. *Palaeogeogr. Palaeoclimatol. Palaeoecol.* **238,** 281–301 (2006).

Supplementary Information is linked to the online version of the paper at www.nature.com/nature.

Acknowledgements We thank P. Meijer, S. Giralt, L. Matenco and C. Ayora for comments and criticisms on earlier versions of the manuscript. This work was funded by the Spanish government through the projects ATIZA (CGL2009-09662), TopoAtlas (CGL2006-05493), TopoMed (CGL2008-03474-E/BTE) and Topolberia (CSD2006-00041).

Author Contributions D.G.-C. planned the study, performed the modelling and wrote the paper; A.V. processed and interpreted the seismic data and tomography; and both authors interpreted and discussed the results.

Author Information The source code developed for the calculations can be downloaded from https://sites.google.com/site/daniggcc/research-interests/messinian. Reprints and permissions information is available at www.nature.com/reprints. The authors declare no competing financial interests. Readers are welcome to comment on the online version of this article at www.nature.com/nature. Correspondence and requests for materials should be addressed to D.G.-C. (danielgc@ictja.csic.es).

METHODS

Methods for water flow and erosion calculations. Consider a sill connecting two oceanic basins with a depth $z_s < 0$ (average across the strait; negative means below initial ocean level) and acting as a water gate between a source basin (Atlantic) at level z_0 and a sink basin with a negative water budget (Mediterranean) at level z_1. These levels are shown in Fig. 1. The seaway depth is reduced by tectonic uplift at a rate U in competition with water flow incision, which is assumed to be a power-law function of basal shear stress, τ.

$$\frac{dz_s}{dt} = U - k_b(\tau - \tau_c)^a \quad (1)$$

Both k_b (the erodibility) and a are positive constants. The uplift rate, U, is taken to be constant in all tests, except for in those whose results are shown in Fig. 2, where a negligible acceleration is arbitrarily chosen to force complete closure at $t = 100$ kyr. The unit stream power approach, including water velocity, V, as a multiplying factor of τ in equation (1), has also been tested, but its influence on results is smaller than other factors discussed in this paper. In equation (1), τ_c is the critical shear stress needed for erosion (50 Pa in the reference model[34]). Although different formulations for water-flow-driven erosion are under debate (see, for example, ref. 34), equation (1) is an adequate first approach to a detachment-limited scenario describing an interoceanic sill with a limited supply of abrasive tools. We consider values of a between 1 and 3 (ref. 35). For $a = 1$, k_b ranges from 10^{-5} and 2×10^{-4} m yr^{-1} Pa^{-1} (that of Himalayan schists and sandstones, respectively[36]) to $\sim 10^{-7}$ m yr^{-1} Pa^{-1} (Himalayan metamorphic phyllites and schists[37]) for river bed incision and 18–40 m yr^{-1} Pa^{-1} for unconsolidated soil erosion[38]. For $a = 1.5$, k_b has been estimated at 8×10^{-6} (Mesozoic limestone[39]) and 1.6×10^{-4} m yr^{-1} Pa$^{-1.5}$ (Oligocene flysch[26]). A value of $a = 3$ may be applicable if cavitation takes place[40].

Shear stress, τ, at the sill can be expressed as the product of water density, ρ; the acceleration due to gravity, g; the mean water depth of the channel, $z_s - z_0$; and the slope of the water surface, S, also known as the hydraulic gradient:

$$\tau = \rho g(z_s - z_0)S \quad (2)$$

We assume that $S = (z_1 - z_0)/L$, where $z_1 - z_0$ is the head loss and $L = 100$ km represents the half-width of the Betic–Rifean orogen. To calculate the water flow over the sill and the level of the Mediterranean basins, we use an empirical relationship relating water flow speed (in metres per second) with the hydraulic gradient (Manning's formula):

$$V = \frac{1}{n} R_h^{2/3} S^{1/2} \quad (3)$$

Here $n = 0.05$ is the roughness coefficient and R_h is the hydraulic radius (in metres) of the strait connecting the Atlantic and the Mediterranean. The hydraulic radius is a measure of the flow efficiency of a river channel, and because channel width is considerably larger than channel depth, it can be assumed that $R_h \approx z_s - z_0$. We also tested the critical flow condition

$$V = \sqrt{g(z_s - z_0)} \quad (4)$$

as an alternative to equation (3), but this does not introduce qualitative changes in the results.

Water discharge (in cubic metres per second) can be calculated as

$$Q = W(z_s - z_0)V \quad (5)$$

where W is the width of the channel (in metres). An empirical relationship for channel width derived from river channel studies[41] has been used:

$$W = k_w Q^{a_w} \quad (6)$$

where $a_w = 0.5$ is an empirically determined constant and $k_w = 1.2$ is a value comparable to mountain rivers and to the channel excavated during the Zanclean flood[26]. However, the models in this paper adopt a more sophisticated form for the width–discharge relationship, accounting for the effect of uplift as derived in ref. 42:

$$W = C_w \left(\frac{\tau_c + U/k_b}{\rho g} \right)^{-3/13} (nQ)^{6/13} \quad (7)$$

Here C_w is an empirically determined constant. Width adjustment to discharge might actually take between thousands and millions of years (see, for example, ref. 34). We assume here that this adjustment is instantaneous, but an extreme case in which the time lag is infinite (that is, the width is constant) yielded similar results, except for a ~20% reduction of the amplitude of the tectonic–erosional oscillations.

The level of the Mediterranean changes as a function of sea evaporation, E; precipitation, P; river supply, R; and Atlantic inflow, Q, above the seaway:

$$\frac{dz_1}{dt} = P - E + \frac{R + Q(z_s, z_0, z_1)}{A_{Med}(z_1)} \quad (8)$$

Here $z_0 - z_1$ is the head loss across the seaway and $A_{Med}(z_1)$ is the surface area of the Mediterranean as a function of its level (hypsometric reconstruction[40]). We use the values $E = 1.2$ m yr^{-1}, $P = 0.6$ m yr^{-1} and $R = 4{,}500$ and $12{,}000$ m^3 s^{-1} for the eastern and western basins, respectively[5,40], consistent with a hydrological deficit nearly 50% smaller than at present[27]. Both basins start at present sea level ($z = 0$). The role of the Sicily sill (taking its present depth to be 430 m) is accounted for as described in ref. 22. Its depth acts as a limit to the sea-level oscillation of the western Mediterranean (Fig. 3), supporting the interpretation (see ref. 28 and references therein) that the erosional terraces formed at similar depths could be related to a moderate sea-level drop during stage 1.

Interdependence between the Mediterranean sea level and the erosion rate results in a harmonic oscillatory behaviour. When levels in both oceanic domains are similar, erosion rates at the sill are low (equations (2) and (3)), implying a shallowing of the seaway, a decrease of inflow and a lowering of Mediterranean level by evaporation. As this level becomes low enough, the large head loss triggers high erosion rates of the sill, leading to large inflow and restoring the level of the Mediterranean. Oscillations occur because evaporation has a delayed effect on level drawdown relative to inflow changes. The frequency and amplitude of these oscillations are mostly dependent on the hydrological deficit involved in equation (6) and on the erodibility, k_b, which determines the amount of head loss required to overcome seaway uplift in equation (1).

Equations (1)–(8) are numerically solved using an explicit finite-difference, time-iterative technique. We use a time step of 0.2 yr and assume that the initial sill depth is $z_s = -60$ m, where the initial ocean level relative to which z_s is measured is taken to be $z_0 = 0$. Increasing the initial sill depth induces only a delay in the time required for closure, which remains otherwise unaffected. Our study cannot discriminate whether this seaway uplift is related to a global sea-level fall or to tectonic uplift of the Gibraltar strait. On complete disconnection, we obtain equilibrium desiccation levels for the Mediterranean basins of $z_1 = 2{,}500$ (west) and $z_2 = 2{,}700$ m (east) below sea level[43]. Global sea level rises 9.5 m as a result of the desiccation, because the water evaporated from the Mediterranean is transferred to the global ocean. The parameterization of the model is shown in Fig. 3 and Supplementary Figs 2 and 3.

Methods for salt budget calculations. To estimate salt precipitation, we track the content of gypsum and halite in Mediterranean water. We take into account the salt input through the inflow current and consider vertically averaged salinity values for the Atlantic, the western Mediterranean and the eastern Mediterranean. The aim of this salt budget calculation is only to check the ability of the tectonic–erosional sea-level oscillations to cause oscillations in salt precipitation comparable to those observed in the marginal basins. More detailed models of Messinian salt precipitation can be found in refs 4, 21, 22. Salinities are here vertically averaged, neglecting brine stratification. We account for salt transport starting with initial gypsum and halite concentrations the same as those in the present ocean: 0.0031 and 0.035 kg l^{-1}, respectively. As the brine concentrates in the Mediterranean, precipitation of gypsum and halite occurs when the total concentration of salt reach 0.140 and 0.3715 kg l^{-1}, respectively. In the absence of mixing between the Atlantic and the Mediterranean, the salt accumulated during the MSC could be precipitated in only 80,000 yr (assuming a Mediterranean water deficit of half the present value, 2.4×10^{12} m^3 yr^{-1}; refs 22, 44). Higher mixing rates would imply a larger time lag before salt precipitation starts and a larger time lag between gypsum and halite precipitation.

We can estimate the sill depth required to cancel outflow by calculating the minimum sill depth that allows an inflow equal to the net evaporation of the Mediterranean (the reasoning is similar to that in fig. 7 in ref. 21). The inflow over such sill is maximized by the critical flow (that is, assuming a drawdown of the Mediterranean level below that of the sill). By using the critical flow condition (equation (4)), assuming the width of this inflowing hypothetical 'cascade' to be five times its depth (a value representative of incising mountain rivers) and using equation (5), it is straightforward to obtain a depth of 22.5 m. This is a minimum estimation of the sill depth cancelling outflow and mixing, because a nearly full Mediterranean slows the inflow (see, for example, ref. 44). The model-calculated sill is shallower than that value during the tectonic–erosional competition, showing that double flow did not occur during that stage. For the initial time steps (before the tectonic–erosional dynamic equilibrium), we used a simple mixing approach whereby Atlantic–Mediterranean mixing varies linearly with depth, between the present mixing rate (1.4% per year[44]) for the present sill depth (284 m) and zero mixing for a depth of 30 m. This only slightly delays (by up to 15 kyr, depending on the uplift rate) the time of saturation of the Mediterranean brines, but does not affect the period or amplitude of the cycles later on. Although there are more refined formulations of the double-sided seaway circulation due to

the salinity difference[44], these do not account for a large drawdown, which is the main drive during the MSC. Previous models have addressed in more detail the role of Atlantic–Mediterranean mixing[4] and the role of vertical stratification within the Mediterranean[45].

Isostatic vertical motions at the seaway related to sea-level changes[20] are not taken into account because they take place over periods of ~20,000 yr imposed by asthenospheric viscosity, and therefore do not affect the shorter oscillation periods derived here.

34. Attal, M. *et al.* Testing fluvial erosion models using the transient response of bedrock rivers to tectonic forcing in the Apennines, Italy. *J. Geophys. Res.* **116,** F02005 (2011).
35. Whipple, K. X. & Tucker, G. E. Dynamics of the stream-power river incision model; implications for height limits of mountain ranges, landscape response timescales, and research needs. *J. Geophys. Res. B* **104,** 17661–17674 (1999).
36. Lavé, J. & Avouac, J. P. Fluvial incision and tectonic uplift across the Himalayas of central Nepal. *J. Geophys. Res.* **106,** 26561–26591 (2001).
37. Wobus, C. W. Heimsath, A. M., Whipple, K. X. & Hodges, K. V. Active out-of-sequence thrust faulting in the central Nepalese Himalaya. *Nature* **434,** 1008–1011 (2005).
38. Elliot, W. J., Liebenow, A. M., Laflen, J. M. & Kohl, K. D. *A Compendium of Soil Erodibility Data from WEPP Cropland Soil Field Erodibility Experiments 1987 & 88.* NSERL Report 3 (Ohio State Univ. and USDA Agricultural Research Service, National Soil Erosion Research Laboratory, 1989).
39. Attal, M., Tucker, G. E., Whittaker, A. C., Cowie, P. A. & Roberts, G. P. Modeling fluvial incision and transient landscape evolution: influence of dynamic channel adjustment. *J. Geophys. Res.* **113,** F03013 (2008).
40. Whipple, K. X. & Hancock, G. S. River incision into bedrock: Mechanics and relative efficacy of plucking, abrasion and cavitation. *Geol. Soc. Am. Bull.* **112,** 490 (2000).
41. Whipple, K. X. Bedrock rivers and the geomorphology of active orogens. *Annu. Rev. Earth Planet. Sci.* **32,** 151–185 (2004).
42. Turowski, J. M., Lague, D. & Hovius, N. Cover effect in bedrock abrasion: a new derivation and its implications for the modelling of bedrock channel morphology. *J. Geophys. Res.* **112,** F04006 (2007).
43. Meijer, P., Th., Slingerland, R. & Wortel, M. J. R. Tectonic control on past circulation of the Mediterranean Sea: a model study of the late Miocene. *Paleoceanography* **19,** PA1026 (2004).
44. Bryden, H. L. & Stommel, H. M. Limiting processes that determine basic features of the circulation in the Mediterranean Sea. *Oceanol. Acta* **7,** 289–296 (1984).
45. de Lange, G. J. & Krijgsman, W. Messinian salinity crisis: a novel unifying shallow gypsum/deep dolomite formation mechanism. *Mar. Geol.* **275,** 273–277 (2010).

doi:10.1038/nature10651

Salt precipitation and sea level changes in the Mediterranean

The model is consistent with a synchronous onset of salt precipitation over the entire Mediterranean basin[1] and compatible with the bull-eye plan-view distribution of salts[46], with halite occupying the central, deeper parts of the basin and gypsum extending closer to the margins (Fig. 1). During the drawdown stage of the cycles, salt concentration increases, eventually inducing halite precipitation only in the deeper parts of the basin (Fig. 2). In contrast, at high water flow, salt concentration decreases while remaining above gypsum saturation, and therefore the gypsum contained in the inflowing Atlantic waters is precipitated as it mixes with the Mediterranean brine (Fig. 1 and Fig. 2). The sea-level drawdown associated to the competition between uplift and erosion of the sill, regardless of the occurrence of cyclicity, ranges between tens and a few hundreds of meters, consistent with the gypsum deposits present in shallow marginal basins. This moderate drawdown might be responsible for the first stage of moderate incision along the Rhone Messinian canyon[28,47].

Model parameterization

We have performed a sensitivity analysis of the main parameters of the model, apart from the one shown in Fig. 3. The effect of incorporating precessional cyclicity in the climatic parameters (precipitation and evaporation) is shown in Fig. SI-3, panels *a* and *b*. Precession cycles seem to exert only minor changes to the cycles formed by tectonic-erosional coupling, because the 21-kyr variations that it implies in the hydrological balance of the Mediterranean have a longer period than the response time of sill erosion. In contrast, the effect of adding cyclic variations of the global sea level relative to the

reference model (shown in the same figure, panels *c*-*e*) is more significant because the higher frequency of these changes outpaces seaway erosion.

Seismic tomography of the upper mantle

To obtain the tomographic images shown in Fig. 4, we use the technique of the P-wave global tomographic model of ref. (*48*), improved with additional arrival times from well-located earthquakes at both teleseismic and regional distances[30]. The new dataset incorporates additional earthquakes from 1995 to 2002 listed in the bulletins of the International Seismological Centre, and arrival times recorded at regional distances that were not used previously. In total, more than 14 million arrival times from 300,000 earthquakes (nearly 4 times the amount used in ref. *48*) were reprocessed using the EHB methodology[49]. The ray paths corresponding to these new arrival times sample mainly the uppermost mantle and it is in this region where the resolving power of the new dataset is increased, allowing to image seismic velocity anomalies of the same resolution of the grid used for the tomographic inversion (0.5ºx0.5º in area and 25-50 km in depth).

Seismicity, isostasy and vertical motions in the Gibraltar Arc

Beyond seismic imaging, the presence of a subcrustal load underneath the westernmost part of the Gibraltar Arc is supported by isostatic studies showing that the flexure of the Iberian Plate under the western Betics needs extra load apart from the emplacement of the orogen[50] and that geoid and gravity data can be better explained by a thicker lithosphere under the area where tomography shows the slab attached to the crust[51].

A recent seismological study[52] shows active crustal deformation to the West and relative quiescence to the East of the present location undergoing lithospheric tearing, as proposed in this paper (Fig. 4 and Fig. SI-4). Tear propagation below the Betics[8] towards Gibraltar is a process capable of causing first the observed uplift of the corridors[53,54] that caused the closure of the Mediterranean and then subsidence at Gibraltar leading to the Zanclean flood. However, our study cannot exclude that closure could have taken place either along the Rifean corridor or even at the Gibraltar Strait.

References in the Supplementary Information

46. K. J. Hsü, M.B. Cita, W. B. F. Ryan, The origin of the Mediterranean environments, *Initial Report of the Deep Sea Drilling Project*, vol. **13**, US Government Print. Office, Washington, 1203–1235 (1973).

47. J. Gargani,Modelling of the erosion in the Rhone valley during the Messinian crisis (France). *Quaternary International* **121**, 13-22 (2004).

48. H. Bijwaard, W. Spakman, E. R. Engdahl, Closing the gap between regional and global travel time tomography. *J. Geophys. Res*. **103**, 30055-30078 (1998).

49. E. R. Engdahl, R. D. van der Hilst, R. P. Buland, Global teleseismic earthquake relocation with improved travel times and procedures for depth determination. *Bull. Seism. Soc. Am.* **88**, 722-743 (1998).

50. D. Garcia-Castellanos, M. Fernàndez, M. Torné, Modelling the evolution of the Guadalquivir foreland basin (South Spain). *Tectonics* **21** (2002), doi:10.1029/2001TC001339

51. J. Fullea, M. Fernàndez, H. Zeyen. Lithospheric structure in the Atlantic–Mediterranean transition zone (southern Spain, northern Morocco): a simple

approach from regional elevation and geoid data. *Comptes Rendus Geosc.* **338**, 140–151 (2006).

52. A. Ruiz-Constán, D. Stich, J. Galindo-Zaldívar, J. Morales, Is the northwestern Betic Cordillera mountain front active in the context of the convergent Eurasia-Africa plate boundary? *Terra Nova* **21**, 352-359 (2009), doi:10.1111/j.1365-3121.2009.00886.x.

53. L. Iribarren, J. Vergés, F. Camurri, J. Fullea, M. Fernàndez. The structure of the Atlantic-Mediterranean transition zone from the Alboran Sea to the Horseshoe Abyssal Plain (Iberia–Africa plate boundary). *Marine Geology* **243**, 97-119 (2007).

54. M. Esteban, J.C. Braga, J. Martín, C. de Santisteban, Western Mediterranean reef complexes. In: Models for Carbonate Stratigraphy from Miocene Reef Complexes of Mediterranean Regions (eds. Franseen, E. K., Esteban, M., Ward, W. C. & Rouchy, J.-M.). Soc. Econ. Paleontol. Mineral., *Concepts in Sedimentol. Paleontol. Ser.* **5**, 55-72 (1996).

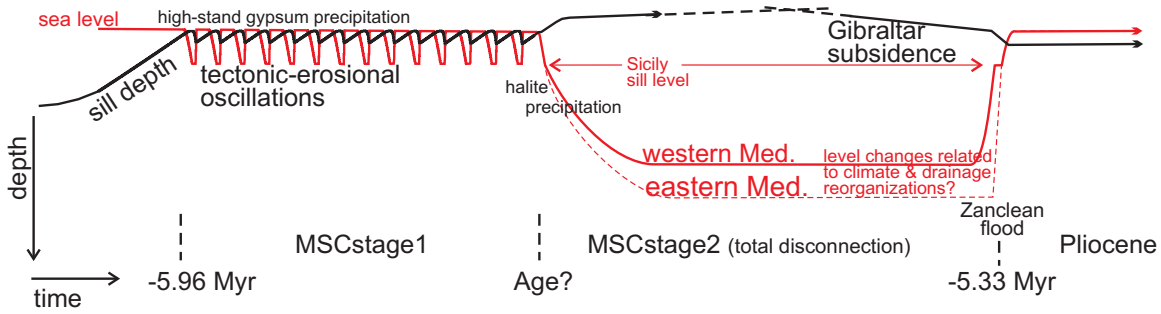

Fig. SI-1.- Conceptual model for the evolution of the Messinian salinity crisis. Stage 1 implies a drawdown of a few hundred meters or less related to the competition between seaway uplift and erosion. This stage may undergo significant cyclicity in water level; Stage 2 starts when erosion is defeated by uplift, and would involve a kilometric drawdown; Later subsidence and possibly erosion of the Gibraltar Sill leads to the overspill and flooding of the Atlantic into the Mediterranean[26]. This model does not involve diachronism between marginal and central basins.

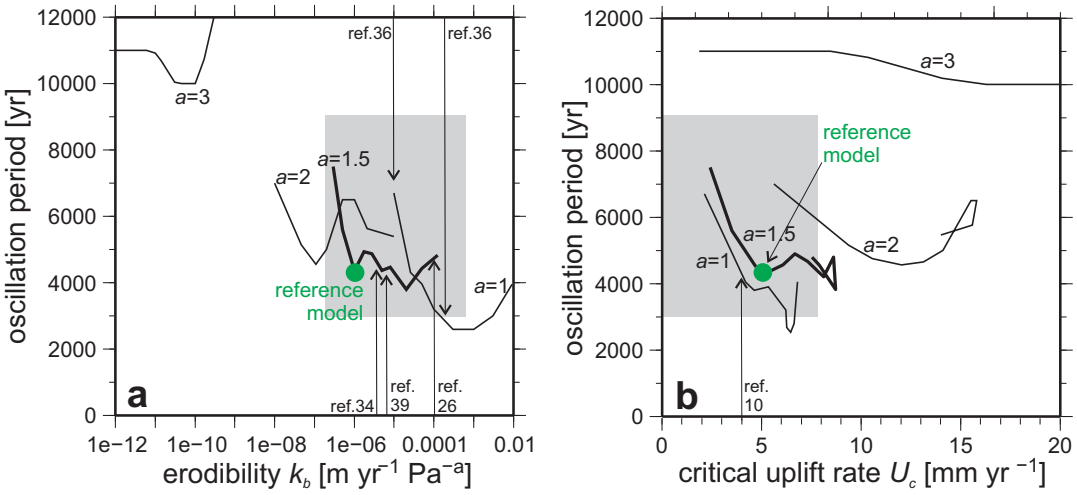

Fig. SI-2. Parameterization of the model of uplift-erosion competition. a) Period of sea level oscillations obtained at critical uplift rates (at the limit of closure) for a range of values of erodibility k_b. b) Period of sea level oscillations as a function of the critical uplift rate, obtained by varying erodibility. Labelled arrows indicate references for erodibility and uplift rates (*Supplementary Information*). Grey-shaded areas indicate the parameter ranges supported by the references and the model results.

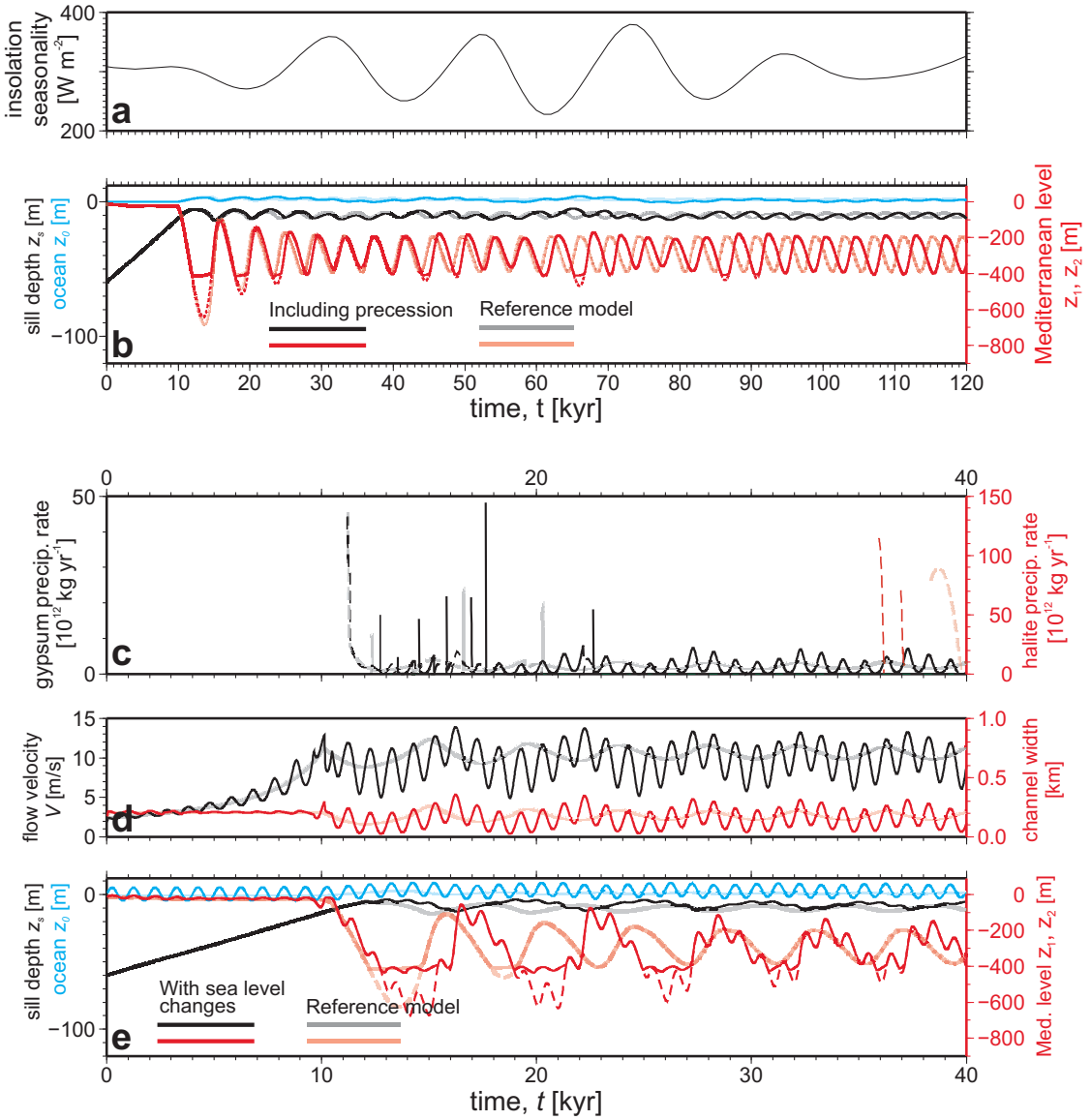

Fig. SI-3. Effects on the model results of precessional insolation changes and global sea level changes. a) Milankovitch changes of insolation during the Messinian (summer-winter variability at 36º N); b) Effect on the reference model of taking *E*, *P* proportional to insolation seasonality. Light lines correspond to the reference model in Fig. 2 (without uplift acceleration). These results suggest that the effect of insolation variability is smaller than that of tectonic-erosional cyclicity in terms of salt precipitation cycles, but note that this is subject to the uncertainty in the conversion between insolation and *E*, *P* values. c)-e) Effect of applying periodic global sea level changes to the evolution of the reference model (shown with light lines for comparison). In this example, an oscillation of a 1000 yr period and 10 m amplitude is applied to the Atlantic Ocean level. This adds a higher frequency oscillation to the tectonic-erosional oscillation, potentially triggering shorter salt precipitation cycles as predicted in ref. 4.

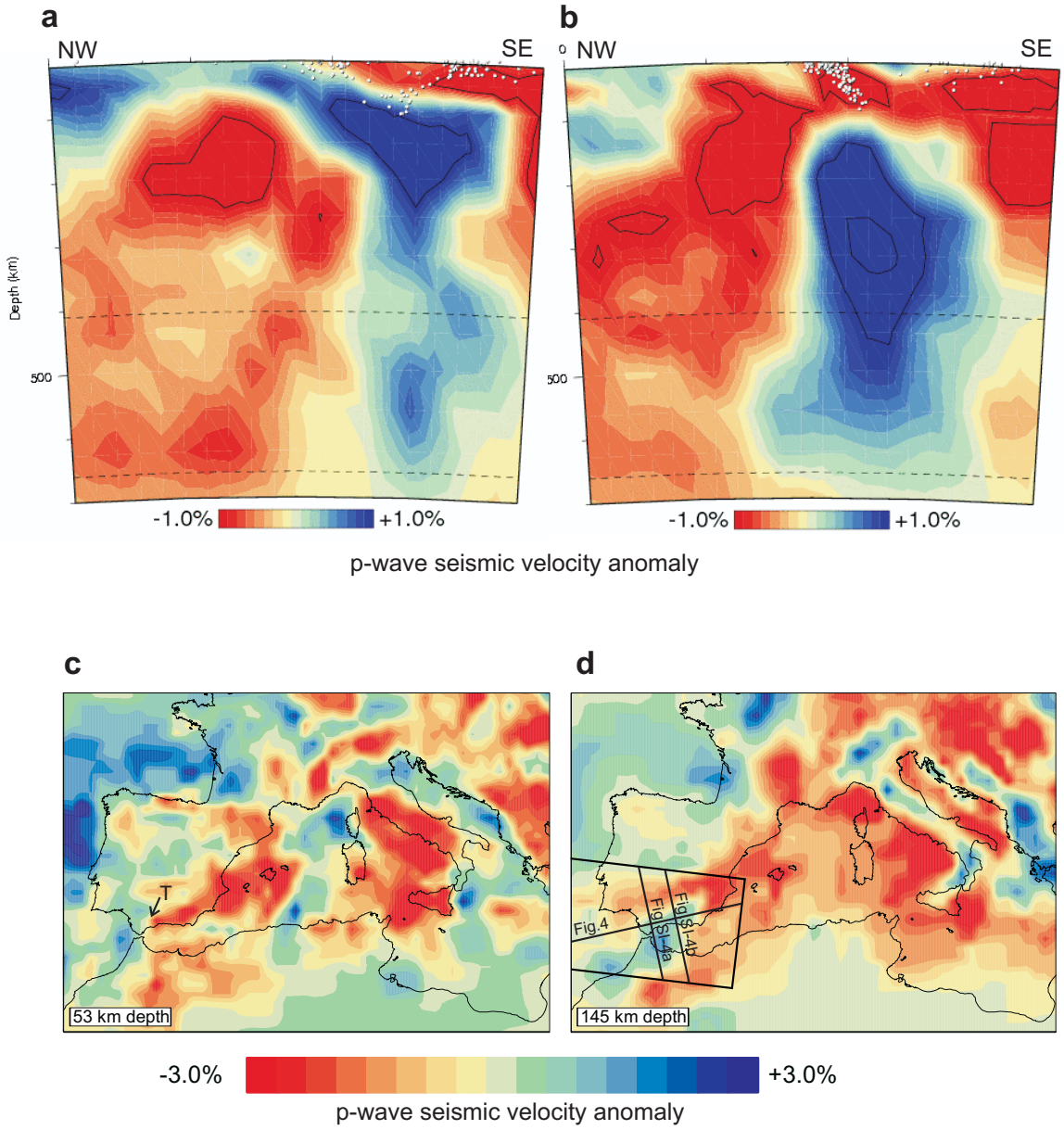

Fig. SI-4. Results from the seismic tomographic inversion. a) Vertical tomographic profile parallel to that in Fig. 4, 110 km to the south, showing the slab detached in the eastern Betics, and attached in the west; b) and c) Horizontal slices of the tomographic model at 53 and 145 km depth, showing the location of profiles in a) and in Fig. 3. The slab (characterised by high seismic velocities depicted in blue) has continuity towards the East at 145 km depth, while at shallower depths it appears replaced by lower-velocity material, suggesting that the slab is detached from the crust in that area, and replaced by asthenosphere. The location of lithospheric tearing is indicated by '*T*'.